Measurement of Cross Sections with Neutrons as Targets*

M. WIDGOFF SHAPIRO
Brown University, Providence, Rhode Island

A. M. CORMACK
Tufts University, Medford, Massachusetts

AND

A. M. KOEHLER
Harvard University, Cambridge, Massachusetts

(Received 12 January 1965)

The purpose of the experiment described in this report was to test the use of the Chew-Low extrapolation technique for the measurement of cross sections with unstable particles as targets. The test was performed by using the Chew-Low method to measure proton-neutron total cross sections σ_{pn} with protons of 161-MeV energy incident on deuterium, and comparing the results thus obtained with values of the neutron-proton cross section previously determined from the scattering of projectile neutrons on hydrogen targets. At two values of the effective incident energy, 125 and 168 MeV, the values found were $\sigma_{pn}=42.9\pm5.6$ mb and $\sigma_{pn}=40.9\pm5.9$ mb, respectively. These values are in sufficiently good agreement with the corresponding values of σ_{np}, particularly at the higher energy where the extrapolation distance is shorter, to give confidence in the Chew-Low method for the determination of unknown cross sections.

I. INTRODUCTION

THE prospect of doing experiments with unstable particles as targets is fascinating although apparently not physically possible. Because of our inability to construct a target of neutrons or pions, such interactions as neutron-neutron, pion-pion, and pion-neutron cannot be studied directly. Cross sections for interactions with neutrons as targets have been determined by taking differences between cross sections measured separately with targets of deuterium and hydrogen. In a similar way, the virtual pions associated with nucleons can be regarded as targets within targets, but in this case the binding effects which obscure the two-body interaction of interest are much more severe than in the deuteron case.

In 1959, Chew and Low[1] proposed a method for analyzing experiments with complex particles as targets so as to obtain the cross section for scattering of the projectile particle by an individual elementary constituent of the complex target. Under the assumptions made by Chew and Low, the resulting two-body cross sections are free of binding effects.

Because of the interesting possibilities of the Chew-Low technique, a number of experiments have been performed which make use of it. A determination of the cross section for $\gamma+n\rightarrow\pi^-+p$ has been made by this method,[2] and it has been used in several measurements of π-π interaction cross sections.[3] Some efforts have been made to check the method: Smith *et al.*[4] used it to remeasure the known cross sections for π^+-p scattering. Because of the problem of insufficient statistics, they were able only to ascertain that two values of the cross section, each averaged over a large energy region, had approximately the correct relative magnitude. Kuckes, Wilson, and Cooper[5] have also studied the use of the deuteron as a free neutron target, but they did not check the Chew-Low method for determination of total cross sections.

The purpose of the experiment described in this paper was to test the Chew-Low theory by using it to determine the total proton-neutron interaction cross section, σ_{pn}, and comparing the value so obtained with σ_{np}, the cross section for interaction of projectile neutrons with target protons.

II. THE CHEW-LOW EXTRAPOLATION METHOD

Consider the interaction

$$p+d\rightarrow p+p+n. \tag{1}$$

This can be represented by the diagram in Fig. 1.

There is here a single-particle intermediate state corresponding to a neutron. Chew and Low conjecture (a) that there is a pole in the S matrix for this diagram at a point related to the mass of the neutron. They further conjecture (b) that the residue at this pole is given by the product of the smaller dimensional S-matrix elements which connect the two groups of particles respectively to the intermediate particle on its

* The work at Brown University was assisted by the U. S. Atomic Energy Commission and the National Science Foundation; the work at Harvard University by the U. S. Office of Naval Research; and the work at Tufts University by the Atomic Energy Commission.

[1] G. F. Chew and F. E. Low, Phys. Rev. **113**, 1640 (1959).

[2] W. P. Swanson, D. C. Gates, T. L. Jenkins, and R. W. Keeney, Phys. Rev. Letters **5**, 339 (1960).

[3] D. D. Carmony and R. T. Van de Walle, Phys. Rev. **127**, 959 (1962); J. A. Anderson, V. X. Bang, P. G. Burke, D. D. Carmony, and N. Schmitz, Phys. Rev. Letters **6**, 365 (1961) and Rev. Mod. Phys. **33**, 431 (1961); E. Pickup, D. K. Robinson, and E. O. Salant, Phys. Rev. Letters **7**, 192 (1961).

[4] G. A. Smith, H. Courant, E. Fowler, H. Kraybill, J. Sandweiss, and H. Taft, Phys. Rev. Letters **5**, 571 (1960).

[5] A. F. Kuckes, Richard Wilson, and P. F. Cooper, Jr., Ann. Phys. (N. Y.) **15**, 193 (1961).

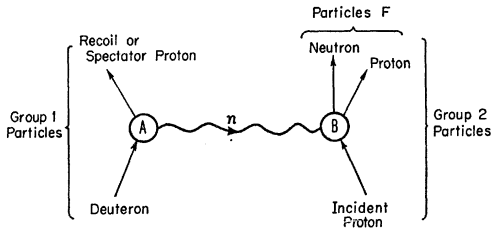

FIG. 1. Diagram of the reaction $p+d\rightarrow p+p+n$ with the neutron as a single particle state linking particles of group 1 and group 2. The vertex B represents the interaction of interest: $p+n\rightarrow p+n$.

mass shell. The matrix element at vertex A is that for the transition $d\rightleftarrows n+p$ and this is known to be directly related to the normalization of the asymptotic wave function of the deuteron. Finally, Chew and Low conjecture (c) that the matrix element connecting the particles of group 2 to the intermediate particle (at vertex B) is equal to the physical matrix element for the interaction between the incoming proton and the intermediate particle to yield the particles F. At the pole, the proton in the deuteron acts as a noninteracting spectator.

Let M_p be the mass of the proton; T_{2L} the laboratory system kinetic energy of the recoil proton; θ_L the laboratory angle of the recoil; then $p^2=2M_pT_{2L}$ is the nonrelativistic momentum of the recoil, squared. Also, let q_{1L} be the laboratory momentum of the incoming proton; M_d, the mass of the deuteron; M_n, the mass of the intermediate particle (the neutron); w, the total energy of particles F (which include all the outgoing particles except the recoil or spectator) in their c.m. system.

In accordance with conjecture (a), the pole in the S matrix occurs at $P^2=-M_n^2$, where P^2 is the square of the total energy-momentum four vector for each of the sets of particles labeled group 1 and group 2 in Fig. 1. It is convenient however to carry out the calculation in terms of the variables p^2 and w^2. Then the pole occurs at

$$p^2=p_0^2=-\left(\frac{M_p}{M_d}\right)[M_n^2-(M_p-M_d)^2]\,, \qquad (2)$$
$$=-0.2091\times10^4(\mathrm{MeV}/c)^2$$

a negative, nonphysical value of p^2. The residue $F(w^2,p_0^2)$ at this pole is found by extrapolating into the nonphysical region to $p^2=p_0^2$, at fixed w^2, the experimentally determined function

$$F(w^2,p^2)$$
$$=2\pi\left(\frac{M_d}{M_p}\right)^2\frac{q_{1L}^2(p^2-p_0^2)^2}{[\frac{1}{4}w^4-\frac{1}{2}w^2(M_n^2+M_p^2)+\frac{1}{4}(M_n^2-M_p^2)^2]^{1/2}}\times\frac{\partial^2\sigma}{\partial(w^2)\partial(p^2)}. \qquad (3)$$

Then we have, through conjectures (b) and (c):

$$F(w^2p_0^2)=\frac{4}{M_p}\frac{\alpha}{1-\alpha r_0}\sigma_{pn}(w)=(1/K)\sigma_{pn}\,, \qquad (4)$$

where $2\alpha/(1-\alpha r_0)=C^2$, the square of the normalization of the asymptotic deuteron wave function, α is the inverse deuteron radius ($=23.18\times10^{11}$ cm^{-1}) and r_0 is the n-p triplet effective range ($=1.74\times10^{-13}$ cm).[6] The pole occurs at $p^2=p_0^2=-\alpha^2$.

Now,

$$w^2=(\omega_{1L}+M_d-M_p-T_{2L})^2-(q_{1L}^2-2q_{1L}p_{2L}\cos\theta_L+p_{2L}^2)\,, \qquad (5)$$

with ω_{1L} and q_{1L} the total laboratory energy and momentum, respectively, of the incoming particle, p_{2L} the momentum of the recoil proton, and the other symbols as defined above. We see that by measuring the energy and direction of a recoil proton, we can obtain $p^2=2M_pT_{2L}$ and w^2. From the two-dimensional distribution in p^2 and w^2 of the recoil particles, we determine $\partial^2\sigma/\partial(p^2)\partial(w^2)$, and calculate $F(w^2,p^2)$.

Since the function F must be extrapolated to a negative value of p^2, it is clearly important to measure $\partial^2\sigma/\partial(p^2)\partial(w^2)$ at the lowest possible values of p^2. In the deuteron case, the allowable phase space for the spectator particle includes $p^2=0$, so that only experimental problems affect the measurement of low values of p^2.

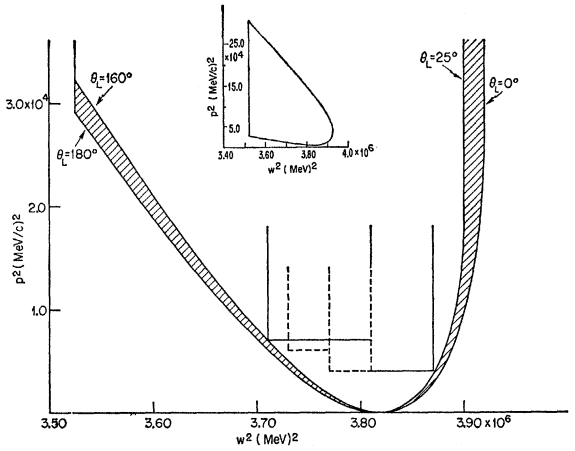

FIG. 2. Phase space available to a proton from the interaction $p+d\rightarrow p+p+n$, for incoming protons of 161 MeV. The variable p^2 is the square of the nonrelativistic momentum of one of the protons (the spectator), while w^2 is the total energy available in the center-of-mass system of the other proton and the neutron. The total available phase space is shown in the inset, while the portion of interest, where p^2 is small, is shown enlarged. The geometry of this experiment was such that events in the shaded region could not be observed.

III. KINEMATICS OF THE INTERACTION

The experiment was performed at the Harvard synchrocyclotron, with a beam of 161-MeV protons.[7] The

[6] Richard Wilson, *The Nucleon-Nucleon Interaction* (Interscience Publishers, Inc., New York, 1963).

[7] F. C. Maienschein and T. V. Blosser, Oak Ridge National Laboratory Report ORNL-3457, 1963 (unpublished).

phase space available in this case to an outgoing proton of interaction (1), in terms of p^2 and w^2, is illustrated in Fig. 2. The total energy in the over-all center-of-mass system is

$$W=(2M_d\omega_{1L}+M_d^2+M_p^2)^{1/2}. \quad (6)$$

The upper limit of w is then $W-M_p$, while the lower limit is M_p+M_n. The upper and lower limits of p^2 depend on both W and w. The allowed region is bounded by $w^2=w_{\min}^2$, and by the w^2 versus p^2 curves for $\theta_L=0°$ and $\theta_L=180°$. For every intermediate value of θ_L, there is a corresponding curve in the allowed region. Two of these are shown in Fig. 2.

If one detected protons of all energies and angles and integrated $\partial^2\sigma/\partial(p^2)\partial(w^2)$ over the entire allowed region, one would obtain the total cross section for interaction (1). Of course, that is not what we are interested in at present. Our aim is to determine $F(w^2,p^2)$ as a function of p^2, at fixed w^2. The prescribed extrapolation to $p^2=p_0^2$ will then yield, through Eq. (4), $\sigma_{pn}(w)$. It is at $p^2=p_0^2$ that the binding effects disappear; $F(w^2,p^2)\neq(1/K)\sigma_{pn}$ at other values of p^2.

Figure 2 shows that p^2 approaches zero at a single value of w^2. This value, $w^2=w_0^2$, is

$$w^2=w_0^2=W^2+M_p^2-(M_p/M_d)(W^2+M_d^2-M_n^2). \quad (7)$$

In the deuteron case, w_0 is also the final center-of-mass energy which corresponds (neglecting the binding shift) to the collision of the incident proton with a neutron at rest in the laboratory. Thus, it is at this value of w^2 that the two-particle collision we are interested in is most closely approximated.

IV. EXPERIMENTAL METHOD

(a) Target and Detector

In order to observe low-energy protons from interaction (1) a target of gaseous deuterium was used, with nuclear-emulsion plates as detectors placed around the target volume. Ilford K2 emulsions 400 microns thick were used. These are sensitive to protons of energies up to about 50 MeV. The entire camera-target chamber (Fig. 3) was filled with deuterium, and no wall intervened between target and detector. With deuterium at a pressure of approximately one atmosphere and the emulsion array as shown in Fig. 3, it is possible to detect protons produced in the target volume with $25°\leqslant\theta_L\leqslant160°$ and with energies as low as 1 MeV. A large number of the recoil protons stop in the dense material of the nuclear emulsion, so that their ranges and hence their energies, as well as their directions, can be determined with precision. Particles coming from the target volume have sufficiently small dip angles in the emulsion, and hence sufficiently long potential ranges, that almost all particles of energies smaller than or equal to 20 MeV [$p^2=3.7\times10^4(\text{MeV}/c)^2$] come to rest in the emulsion. The only exceptions are particles which interact in the emulsion, or whose tracks are so flat that multiple scattering causes them to re-emerge from the emulsion surface.

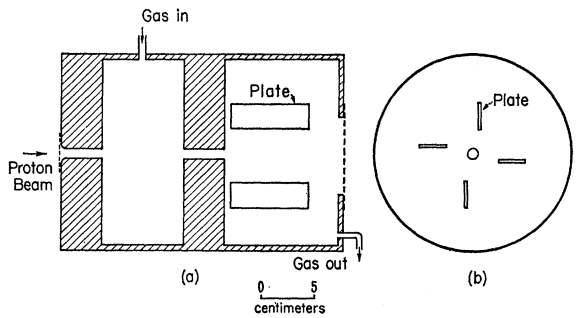

FIG. 3. (a) Schematic diagram of target-camera chamber, showing the final collimating and antiscattering slits, and the plate positions. (b) End view, drawn looking into the beam.

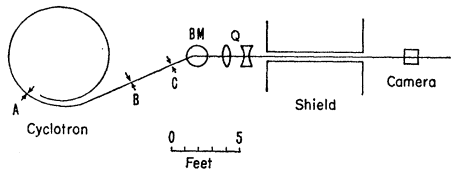

FIG. 4. Path of focused beam of 161-MeV protons from the Harvard cyclotron. A, B, and C are adjustable slits, BM is a bending magnet, Q are quadrupole magnets.

(b) The Proton Beam

The radius of the target volume was set by the cross section of the beam itself. In order to have a well-defined target volume it was necessary that the main part of the beam be contained within a radius small compared with the target-detector distance, and that the beam intensity drop off very rapidly at the radial boundary. This latter requirement was essential in order to reduce the background of tracks from sources other than the target volume, as the target was of such small size and low density compared with the plates themselves and the plate holder. By focusing and collimation a beam has been developed in which the proton flux drops off to 10^{-4}–10^{-5} of the central flux in a full width of about 16 mm. The beam path and camera position are shown in Fig. 4, and the radial profile of the beam at the target is illustrated in Fig. 5. With this beam, a satisfactory signal-to-noise ratio was achieved in the emulsions, and the beam intensity was sufficient to allow exposures of reasonable length—a few hours in duration. This beam also has excellent momentum resolution: $\Delta p/p<\sim0.5\%$.

The proton flux during exposure was measured by means of a nitrogen-filled ion chamber which was calibrated by comparison with a Faraday cup.

The beam alignment and its steadiness during exposure was checked by continuously comparing the signals in the two halves of a split detector placed downstream of the collimator.

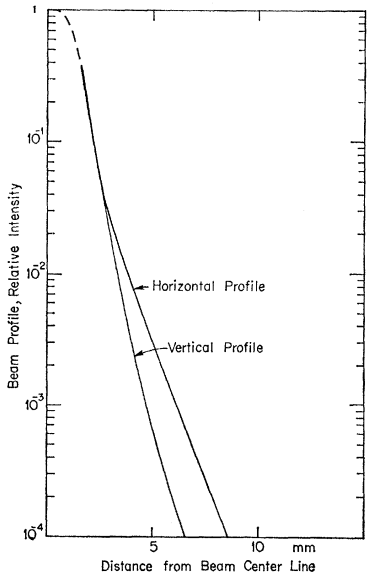

FIG. 5. Profile of beam intensity, in horizontal and vertical directions.

The range of the beam protons in water had been determined by a group from Oak Ridge[7] shortly before the emulsion exposure. Their value of 17.9 g cm^{-2}, with the Barkas range-energy curve for water,[8] gave a proton energy of 161 MeV.

(c) Scanning Procedure

With the emulsions arranged as in Fig. 3, offset from the center of the target volume, and with the target radius set at 4.9 mm, almost all the tracks from the target volume entered the emulsions at their top, or air, surfaces. In order to ease the scanning, only tracks which entered at this surface were accepted. The plates were divided into swathes which were about 80 μ wide and whose length L was almost the full length of the plate (Fig. 6). Individual swathes, each with its fixed target-to-detector distance d, were scanned for particles entering at the air surface. Particles entering from directions such that the target could obviously not be the source were counted but not measured. For all but these obvious cases, the scanner followed each track to determine whether the particle came to rest in the emulsion. Particles which came to rest and those which left the emulsion or interacted in flight were put in separate classes, but in any case the scanner measured for each track its projected length and its depth of penetration in the emulsion, its projected angle at entrance, and its dip angle at entrance.

If the target were infinitely long, recoil protons coming from it at any angle, from 0 to 180°, would be detected in a given swathe. Because of the limited length of the target volume, it can be seen from Fig. 6 that protons at angles $\theta_L<\theta_3=\tan^{-1}[d/(L+a_1)]$ and $\theta_L>\theta_4=\tan^{-1}[-d/(L+a_2)]$ could not be detected at all in a given swathe. The effective target length for these angles was zero. For $\tan^{-1}(d/a_1)=\theta_1<\theta_L<\theta_2=\tan^{-1}(-d/a_2)$ the effective target length was equal to L, while for angles $\theta_3<\theta_L<\theta_1$ and $\theta_2<\theta_L<\theta_4$, the effective target length ranged between 0 and L. This variable geometrical efficiency was taken into account. For the phase-space region of greatest interest the geometrical efficiency was high.

Scanning efficiencies were determined by having pairs of scanners measure the same swathe. The efficiencies ranged from 70–85%. Above a certain minimum track length, no dependence of efficiency on track length was observed. However, inefficiency for counting short tracks and the difficulty of making precise measurements on them made it advisable to set the minimum range at about 40 μ, corresponding to a proton energy of about 2 MeV at entrance in the emulsion. Because of this limitation, the lowest value of p^2 that turned out to be experimentally feasible was $p^2=0.4\times10^4(\mathrm{MeV}/c)^2$.

(d) Background

The background of particles coming from regions outside the target volume was easily eliminated by discarding tracks whose initial directions in the plate did not project back through the target volume. This procedure could not eliminate those particles which originated in material beyond the target, and which then passed through the target on their way to the emulsion. That there was a negligible number of such particles is indicated by the fact that almost no "acceptable" tracks were found in an exposure made with the target chamber evacuated. Internal evidence also showed that a negligible number of particles underwent scattering from one emulsion into another emulsion in the array, especially in directions that could cause them to be taken for particles originating in the target.

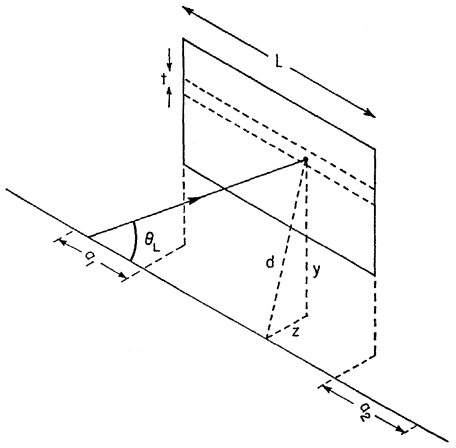

FIG. 6. Position of a scanned swathe of length L and width t, relative to the beam center line, with the trajectory of a particle scattered at the laboratory angle θ_L shown. This diagram defines the quantities t, d, y, z, a_1, a_2, and L used in the text. The length of the target volume is $L+a_1+a_2$.

[8] Walter H. Barkas, Nuovo Cimento 8, 201 (1958).

Another source of background, which could not be eliminated by geometrical considerations, was contamination in the deuterium target. The deuterium was supplied with a purity of 99.7%. The major source of contamination was outgassing from the emulsion material itself. This outgassing rate was reduced to about 11 μ per minute by pumping on the emulsion for two hours before filling the chamber with deuterium for an exposure. Although the outgassing rate could have been reduced still further by longer pumping without damage to the emulsions, any longer pumping time would have seemed excessive. The contamination from outgassing was limited to 1% or less by maintaining a steady flow of fresh deuterium through the target chamber, at the requisite rate.

(e) Data Processing

The information supplied by the scanners was analyzed by means of an IBM-7070 computer. The program was designed to do the following:

(1) Calculate the angle in space θ_L of each track and determine whether or not it is acceptable—i.e., whether or not its direction is consistent with production in the target volume.

(2) Obtain the total range in emulsion and calculate the distance traversed in the gas between the target volume and the emulsion.

(3) Determine the proton energy at the point of production, from the range-energy relation of Barkas[8] for emulsions, and of Barkas[9] for deuterium. In using Ref. 9, the ionization potential of deuterium was taken to be the same as that of molecular hydrogen, $I=19\pm1$ eV.[10] A correction was made for the change in density of the emulsion during pumping and exposure in the dry deuterium. This correction was estimated on the basis of the work of Oliver.[11]

(4) Calculate p^2 and w^2 for each proton, from its energy and θ_L.

(5) Determine the distribution of particles with respect to p^2 and w^2—a two-dimensional distribution.

(6) Calculate the contribution of each track to the function $F(w^2,p^2)$, and sum these contributions to determine $F(w^2,p^2)$.

The relation between F and the distribution determined in step (5) can be seen as follows.

The probability per unit length of target that a proton i will be produced [through interaction (1)], with p_i^2 and w_i^2 lying in the intervals p^2 to $p^2+\Delta p^2$ and w^2 to $w^2+\Delta w^2$, respectively, is equal to $\Delta p^2\Delta w^2\partial^2\sigma/\partial(p^2)\partial(w^2)$. In a cylindrical geometry with a line target, the probability of detecting such a particle in a swathe of width t is $tz/2\pi d^3=tz/2\pi(y^2+z^2)$, with the symbols as they are defined in Fig. 6. If N_p is the number of incident protons and N_V is the number of deuterons per unit volume, then the number of such particles observed in a given swathe, per unit length of target, is

$$N_t(p^2,\,p^2+\Delta p^2;\,w^2,\,w^2+\Delta w^2)=N_pN_V\Delta p^2\Delta w^2(tz/2\pi d^2)\partial^2\sigma/\partial(p^2)\partial(w^2)\,.$$

Since the target volume is not infinite in length, its effective length is a function of θ_L, as described above, and must be determined for each track. Also the target is not really a line target, so z and d are somewhat different for each track. Although they cannot separately be determined exactly, the ratio z/d or z/y can be found from the track in the emulsion. Making use of this ratio, we find

$$\frac{\partial^2\sigma}{\partial(p^2)\partial(w^2)}=\frac{1}{N_pN_V}\frac{2\pi}{t}\frac{y}{\Delta(p^2)\Delta(w^2)}\times\sum_{i=1}^{N_t}\frac{(1+(z_i/y_i)^2)}{L_iz_i/y_i}\,, \quad (8)$$

where y is measured to the beam center. Each track is thus given a weight depending on the geometrical efficiency for detecting it, and the error arising in $\partial^2\sigma/\partial(p^2)\partial(w^2)$ from the uncertainty as to the exact point of origin within the target volume is reduced. Internal evidence of the tracks in the plates indicates that the opposite pairs of plates were, with small error, symmetrically disposed about the actual beam center. Errors arising from any small asymmetry were reduced by summing together the data from opposite pairs of plates.

In terms of the quantities directly measured or calculated for each track i the function F given in Eq. (3) becomes, for a given swathe,

$$F(w^2,p^2)=2\pi\left(\frac{M_d}{M_p}\right)^2q_{1L}{}^2\frac{2\pi y}{N_pN_Vt}\frac{1}{\Delta(p^2)\Delta(w^2)}\frac{1}{\epsilon}\times\sum_{i=1}^{N_t}\frac{(p_i{}^2-p_0{}^2)^2}{[\frac{1}{4}w_i{}^4-\frac{1}{2}w_i{}^2(M_n{}^2+M_p{}^2)-\frac{1}{4}(M_n{}^2-M_p{}^2)^2]^{1/2}}\times\frac{(1+(z_i/y_i)^2)}{L_iz_i/y_i}\,, \quad (9)$$

where N_t is the number of acceptable tracks found in the swathe, in a given Δp^2, Δw^2 interval, and ϵ is the scanning efficiency. The data from the various swathes are combined with account taken of the quantities which could vary from swathe to swathe: ϵ, y, t, and N_p. N_V was maintained at a constant value throughout the exposure.

[9] Walter H. Barkas, University of California Radiational Laboratory Report UCRL 10292, 1962 (unpublished).
[10] U. Fano (private communication.) This value stem as from calculation by Platzman.
[11] Albert J. Oliver, Rev. Sci. Instr. 25, 326 (1954).

(f) Correction for Particles Not Stopping in the Emulsion

All the quantities in (9) can be determined for each particle that comes to rest in the emulsion. However there is also a contribution to the cross section from particles whose total range cannot be measured: particles of more than sufficient energy to penetrate the whole emulsion layer, particles which interact in the emulsion, and particles which undergo multiple scattering in such a way that they leave the emulsion. For each of these the measured track length in the emulsion sets a lower limit on its range and hence on its energy and p^2. By using the distribution in p^2 determined from stopping particles which have a long potential range in the emulsion, it is possible to calculate the relative probabilities for the actual p^2 to lie within various intervals in p^2 above the lower limit for each nonstopping particle. Since the direction of these nonstopping particles can be measured, the values of w^2 corresponding to these intervals in p^2 can also be calculated. A set of kinematically possible $\Delta(p^2)$, $\Delta(w^2)$ intervals is thus established for each nonstopping particle, and a contribution to the cross section $\partial^2\sigma/\partial(p^2)\partial(w^2)$ is calculated for each of these intervals, the contributions being weighted by the relative probabilities of occurrence of the allowed p^2 values.

V. RESULTS AND DISCUSSION

At the point $w^2=w_0^2$, the target neutron is at rest in the over-all laboratory system, and hence the condition of a two-body proton-neutron interaction in the laboratory is most closely approached. Since $F(w^2,p^2)$ cannot be found at a point value of w^2, it is necessary to group together the particles occurring in a finite interval Δw^2. This is equivalent to averaging over the corresponding range of Q(=available energy) in the pn system. To obtain the cross section at a well-defined energy, it is desirable to have Δw^2 as small as it can be while still including a sufficient number of tracks to give the result statistical significance. The total w^2 interval available at low p^2 was divided into two sections which are shown by solid lines on the phase space diagram in Fig. 2. The values of $KF(w^2,p^2)$ as functions of p^2 for these two regions are presented in Table I. The tracks have been grouped together in intervals of $\Delta p^2=2.0\times10^3(\mathrm{MeV}/c)^2$. A larger value of Δp^2 was not used because, although it would have been desirable for statistical reasons, it would have obscured the behavior of F at low p^2. Values of KF_1 and N_1, for stopping particles only, are given as well as KF and N which include the corrections for particles that do not come to rest in the emulsion [Sec. IV(f)]. In the geometry of this experiment a particle originating in the stipulated target volume has a minimum potential range of about 1.3 mm in a 400 μ emulsion, and the correction becomes large only for particles of greater range—particles of energy greater than 20 MeV, $p^2>3.7\times10^4(\mathrm{MeV}/c)^2$. At lower p^2 values the corrections arise from particles which interact in the emulsion or are scattered out of the emulsion. In the interval of p^2 used in this analysis, the correction at any point amounted at most to 10% of F.

TABLE I. $KF_1(p^2,w^2)$ and $KF(p^2,w^2)$ versus p^2, for two energy intervals, with F as obtained from Eq. (9) and K defined in Eq. (4). KF_1 and N_1 are the function and the number of tracks entering into its determination, respectively, for stopping particles only. KF and N are the same quantities, with corrections for particles that do not come to rest in the emulsion. The energy intervals are given in terms of the available energy Q in the pn c.m. system and in terms of the corresponding laboratory energy of a proton incident on a free neutron, as well as in terms of w^2.

Energy interval	p^2 Nominal value $[10^4(\mathrm{MeV}/c)^2]$	Δp^2 $[10^4(\mathrm{MeV}/c)^2]$	N_1	N	KF_1 (mb)	KF (mb)
$3.81\times10^6\leqslant w^2<3.87\times10^6(\mathrm{MeV})^2$	0.5	0.4–0.6	167	167.5	79.2± 4.3	79.5± 4.3
$74.2\leqslant Q<89.5$ MeV	0.7	0.6–0.8	132	132.8	89.8± 5.3	90.1± 5.3
$152\leqslant T_{\mathrm{free}}<184$ MeV	0.9	0.8–1.0	117	117.8	124.1± 7.6	125.1± 7.9
	1.1	1.0–1.2	94	95.4	101.6± 6.9	103.0± 7.3
	1.3	1.2–1.4	70	71.4	117.2± 9.6	119.1± 9.6
	1.5	1.4–1.6	64	65.3	141 ±12	143 ±12
	1.7	1.6–1.8	59	60.3	140 ±12	143 ±13
	1.9	1.8–2.0	59	60.3	162 ±14	166 ±15
	2.1	2.0–2.2	50	51.3	129 ±12	133 ±13
	2.3	2.2–2.4	38	39.3	143 ±16	147 ±16
	2.5	2.4–2.6	26	27.3	73.6± 9.9	81.8±10.6
	2.7	2.6–2.8	24	25.3	85.8±11.9	91.4±12.2
$3.71\times10^6\leqslant w^2<3.81\times10^6(\mathrm{MeV})^2$	0.8	0.7–0.9	72	73.5	43.2± 3.3	44.2± 3.6
$48.4\leqslant Q<74.2$ MeV	1.0	0.9–1.1	54	56.0	47.2± 4.3	48.8± 4.3
$98\leqslant T_{\mathrm{free}}<152$ MeV	1.2	1.1–1.3	44	46.6	42.2± 4.3	44.6± 4.3
	1.4	1.3–1.5	45	47.6	77.2± 7.9	81.5± 7.9
	1.6	1.5–1.7	35	38.0	60.1± 6.9	65.3± 7.3
	1.8	1.7–1.9	53	56.0	143 ±13	151 ±14
	2.0	1.9–2.1	47	50.4	131 ±13	140 ±13
	2.2	2.1–2.3	36	39.8	123 ±14	136 ±15
	2.4	2.3–2.5	37	40.8	147 ±16	161 ±17
	2.6	2.5–2.7	34	38.6	153 ±18	174 ±19
	2.8	2.7–2.9	35	39.6	213 ±24	241 ±26

TABLE II. Extrapolation functions and cross section results.

Energy interval $(MeV)^2$	Form of fitted functions	Total interval in p^2 $[10^4(MeV/c)^2]$	Number of points fitted	Number of tracks	Constants of fitted functions a (mb)	b $[10^{-4}mb/(MeV/c)^2]$	c $[10^{-8}mb/(MeV/c)^4]$	χ^2	$P(\chi^2)$[a] (%)	$KF(p_0^2)=\sigma_{pn}(w^2)$ (mb)
$3.81\times10^6\leqslant w^2$ $<3.87\times10^6$	$KF=a+bp^2$	0.4–2.0	8	770.8	52.5	56.1	···	2.1	91	40.9± 5.9
	$KF1=a+bp^2$	0.4–2.0	8	762	53.5	53.8	···	2.1	91	42.2± 5.9
	$KF=a+bp^2+cp^4$	0.4–2.0	8	770.8	52.1	57.1	−0.495	2.1	84	40.3±19.5
	$KF1=a+bp^2+cp^4$	0.4–2.0	8	762.	52.1	57.1	−1.54	2.1	84	40.3±19.1
$3.71\times10^6\leqslant w^2$ $<3.81\times10^6$	$KF=a$	0.7–1.3	3	176.1	45.5	···	···	0.09	95	45.5± 1.0
	$KF1=a$	0.7–1.3	3	170	43.9	···	···	0.09	95	43.9± 1.0
	$KF=a+bp^2$	0.7–1.3	3	176.1	43.2	2.31	···	0.1	75	42.9± 5.6
	$KF1=a+bp^2$	0.7–1.3	3	170	44.2	−1.07	···	0.1	75	45.2± 5.6
	$KF=a+bp^2+cp^4$	0.7–2.9	11	526.9	57.7	−51.8	40.8	14.4	8	70.6±27.1
	$KF1=a+bp^2+cp^4$	0.7–2.9	11	492	54.1	−44.0	35.3	15.2	6	64.7±26.7
$3.77\times10^6\leqslant w^2$ $<3.81\times10^6$	$KF=a+bp^2+cp^4$	0.4–1.4	5	190.3	36.6	−41.1	76.9	0.7	70	48.5±23.1
	$KF1=a+bp^2+cp^4$	0.4–1.4	5	185.	36.3	−38.6	71.6	0.8	67	47.2±23.3
$3.73\times10^6\leqslant w^2$ $<3.77\times10^6$	$KF=a$	0.6–1.6	5	72.0	35.0	···	···	2.4	66	35.0± 2.0
	$KF1=a$	0.6–1.6	5	70	34.0	···	···	1.9	75	34.0± 2.0
	$KF=a+bp^2$	0.6–1.6	5	72.0	24.6	10.8	···	1.7	64	22.4± 7.9
	$KF1=a+bp^2$	0.6–1.6	5	70	26.8	7.39	···	1.8	62	25.4± 7.9
	$KF=a+bp^2+cp^4$	0.6–2.0	7	90.6	42.9	−28.2	19.9	5.1	27	49.5±29.0
	$KF1=a+bp^2+cp^4$	0.6–2.0	7	87	41.6	−24.9	16.7	5.6	23	47.5±29.0

[a] χ^2 has its usual statistical meaning, and the numerical values were calculated from the data and the form of the fitted function. For a particular form of the fitted function, $P(\chi^2)$ is the probability that χ^2 will exceed the numerical value.

The data of Table I are plotted in Fig. 7. The extrapolations were carried out by making least-squares fits to the data.

For $3.81\times10^6\leqslant w^2<3.87\times10^6(MeV)^2$ and $0.4\times10^4\leqslant p^2<2.0\times10^4(MeV/c)^2$ the points are well fitted by either a first-order or second-order polynomial with p^2 as the independent variable. In fact, over the region in question, the quadratic function is indistinguishable from the linear one, but the statistical uncertainty in the extrapolation is much greater in the quadratic case. This can be seen in Table II, where the constants of the fitted functions are tabulated, together with the extrapolated values $KF(p_0^2)=\sigma_{pn}(w)$ [see Eq. (4)]. Figure 7(a) shows that the function F departs markedly from a straight line for $p^2>2.0\times10^4(MeV/c)^2$, so the data beyond this point were not used in the determination of the extrapolation function.

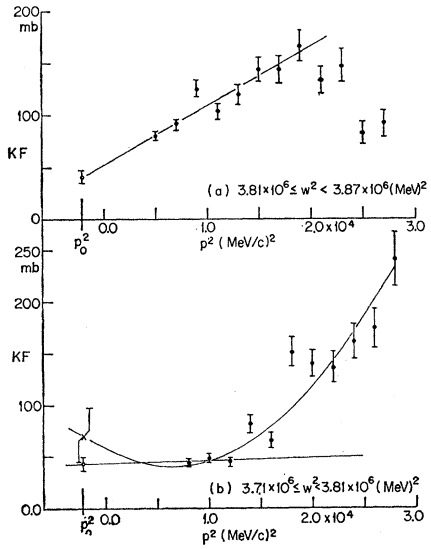

FIG. 7. $KF(p^2,w^2)$ versus p^2 for two intervals in w^2. The curves drawn were found by least-squares fits to the experimental points: The straight line and a second-order polynominal were indistinguishable for the higher w^2 interval up to $p^2=2.0\times10^4$ $(MeV/c)^2$. Beyond this point there is a sharp change in slope, and the data at higher p^2 were not used to establish the extrapolation function. For the lower interval a straight line was fitted to the three lowest p^2 points, where a constant value fits also within the experimental errors. A second-order polynomial fitted over a larger range of p^2 values is also shown. The extrapolations to the points $p^2=p_0^2$, where $KF(p_0^2)=\sigma_{pn}$, are given, with the statistical errors.

In the energy region $3.71\times10^6\leqslant w^2<3.81\times10^6$ $(MeV)^2$, only the first three points, $0.7\times10^4\leqslant p^2<1.3\times10^4(MeV/c)^2$, can be fitted by a straight line. In fact, over this region, the data are consistent with a constant value of F. The cross sections obtained from this constant value and also the extrapolation of a fitted first-order polynomial are given in Table II. Over a larger interval of p^2, a quadratic fit must be made, and the fitted second-order polynomial is also given in Table II. It is clear that if F is assumed to be constant, a result with misleadingly small statistical uncertainty will be obtained.

An alternative subdivision of the larger energy interval is shown by the dashed lines in Fig. 2. For the energy region $3.77\times10^6\leqslant w^2<3.81\times10^6(MeV)^2$ only a quadratic fit is possible, even over the lowest values of p^2, as the slope of the function F decreases with decreasing p^2 over the whole interval studied. The fitted second-order polynomial is given in Table II. Like the other quadratics, this yields an extrapolated value with a large statistical uncertainty. In the energy region $3.73\times10^6\leqslant w^2<3.77\times10^6(MeV)^2$ the values of F for $0.6\times10^4\leqslant p^2<1.6\times10^4(MeV/c)^2$ are consistent with a constant value of F, which is given in Table II. The first subdivision of the data appears to be preferable, because of the large uncertainty in the quadratic fit for $3.77\times10^6\leqslant w^2<3.81\times10^6(MeV)^2$.

Aitchison[12] has discussed in some detail the effects of other poles, arising from final-state interactions, which might tend to obscure the Chew-Low pole. These should be relatively untroublesome at 160-MeV incident energy; they would cause more difficulty at lower

[12] I. J. R. Aitchison, Phys. Rev. 130, 2484 (1963).

energies. Keeping to low p^2 also avoids the region in which final-state interactions become important. The changes in slope seen at higher p^2 may well be connected with the onset of final-state-interaction effects, but the data there are not sufficiently significant statistically to warrant an attempt to fit them quantitatively with a final-state-interaction term.

The errors shown in Fig. 7 and given in Table II are the standard deviations due to counting statistics only. They do not include any estimates of the errors in the various factors that enter into this cross section measurement, as they enter in all cross section measurements: the beam intensity, the target density, the solid-angle factors, and the efficiency of detection. These together contribute a further uncertainty of about 12%. The major source among them is the measurement of z. However, these sources of error do not limit the Chew-Low method any more than they limit a direct measurement of cross section.

The quoted counting statistical errors, on the other hand, represent the inherent difficulties of application of the Chew-Low scheme, as distinct from direct cross section measurements. The required distribution of the particles in a two-dimensional array means that even with a large total number of tracks, the individual values of $\partial^2\sigma/\partial(p^2)\partial(w^2)$ and hence of $F(w^2,p^2)$, have a considerable statistical uncertainty.[13] The extrapolation, except where F can be considered constant, then magnifies this uncertainty.

The cross sections σ_{pn} determined by extrapolation are plotted in Fig. 8 together with a curve showing σ_{np} as a function of the energy of the incoming neutron. This curve was drawn by using the data of Bowen *et al.*[14]; Taylor and Wood[15]; Mott, Guernsey, and Nelson[16]; and Kazarinov and Simonov.[17] The extrapolation at the higher energy, which in fact uses the data from the energy interval near w_0^2, where the two-body collision is most closely approximated, yields a value of σ_{pn} which agrees very well with σ_{np}. The cross section obtained from the data in the lower energy interval is somewhat low compared with the curve, but is still not very bad. Instead of following the curve and increasing by about 30% as the mean energy decreased, the cross section remained constant, within the statistical errors. The two points were plotted at the midpoints of their respective energy intervals, not a a weighted mean energy. Such a weighting would shift the two points somewhat toward each other along the energy axis.

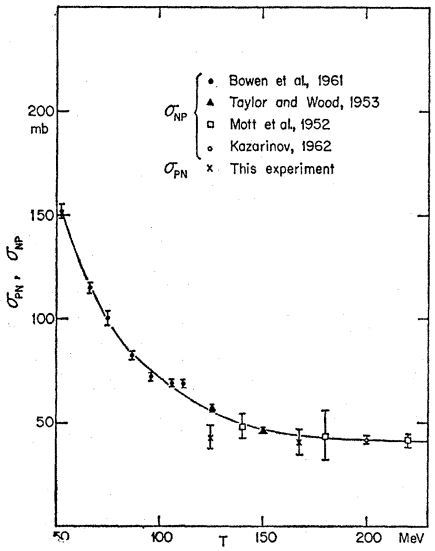

FIG. 8. Comparison of σ_{pn} measured in this experiment using the Chew-Low method, with measurements of σ_{np} in the same energy region. T is the nominal kinetic energy of the incoming particle.

[13] The contributions to the uncertainty in F of errors in measurement of q_{1L}^2, p^2, and w^2 are at most about 2%—much smaller than the statistical uncertainty in $\partial^2\sigma/\partial(p^2)\partial(w^2)$.

VI. CONCLUSION

The Chew-Low extrapolation method has been used to measure σ_{pn} at two energies, corresponding to the midpoints of two energy intervals from which the data were drawn. The cross sections found are $\sigma_{pn}=40.9\pm5.9$ mb and 42.9 ± 5.6 mb, at nominal energies of 168 and 125 MeV, respectively. In spite of the large statistical uncertainties that are practically inescapable in the application of this method, these values agree rather well with σ_{np} measured at the same incoming energies. This is particularly true for the cross section at the higher energy, which is in the neighborhood of $w^2=w_0^2$, where the neutron is effectively at rest in the deuteron and the proton-neutron interaction most closely approximates a two-body interaction in the laboratory. These results confirm the validity of the Chew-Low method, and give confidence in its use to determine unknown cross sections.

ACKNOWLEDGMENTS

It is a pleasure to express our gratitude to all the people who have helped in carrying out this experiment: to the emulsion scanners at Brown University, in particular to Mrs. Dorothy Stepak, for much careful work in scanning and measuring the tracks; to Mrs. Ruth Preist who performed invaluable services in writing the computer programs and in other aspects of the data processing, and to the staff of the Harvard Cyclotron whose cooperation helped greatly in the exposure of the nuclear emulsions.

[14] P. H. Bowen, J. P. Scanlon, G. H. Stafford, and J. J. Thresher, Nucl. Phys. 22, 640 (1961).
[15] A. E. Taylor and E. Wood, Phil. Mag. 44, 95 (1953).
[16] G. R. Mott, G. L. Guernsey, and B. K. Nelson, Phys. Rev. 88, 9 (1952).
[17] Y. M. Kazarinov and Y. N. Simonov, Zh. Eksperim. i Teor. Fiz. 43, 35 (1962) [English transl.: Soviet Phys.—JETP 16, 24 (1963)].